ELSEVIER

Contents lists available at ScienceDirect

Acta Astronautica

journal homepage: www.elsevier.com/locate/actaastro





Complete CASSE acceleration data measured upon landing of Philae on comet 67P at Agilkia

W. Arnold ^{a,*} , M.M. Becker ^b, H.-H. Fischer ^c, B. Ibrahim ^b, M. Knapmeyer ^d, H. Krüger ^e

- ^a Saarland University, Department of Materials Science and Engineering, Saarbrücken, Germany
- ^b Fraunhofer Institute for Non-Destructive Testing (IZFP), Saarbrücken, Germany
- ^c Retired from DLR Microgravity User Support Centre, Cologne, Germany
- ^d DLR Institute of Planetary Research, Berlin, Germany
- ^e Max Planck Institute for Solar System Research, Göttingen, Germany

ARTICLEINFO

Keywords: Rosetta mission Comet 67P Philae landing Impact process CASSE SESAME

ABSTRACT

On November 12th 2014, the Rosetta lander Philae touched down at the site Agilkia on comet 67P. Here, we report unpublished data of the Comet Acoustic Surface Sounding Experiment (CASSE) which belonged to the Surface Electric Sounding and Acoustic Monitoring Experiment (SESAME). The CASSE signals were measured by the accelerometers built-in in the landing feet of Philae. Whereas the acceleration data in the direction perpendicular to the comet surface have been published earlier, the acceleration data measured parallel to the comet surface have been archived until now only on a server of the ESA Planetary Science Archive, and were not further evaluated. However, analyzing the acceleration data with the short-time Fourier-transform allows one to discern the time-sequence of the touch-down of the lander feet at the site Agilkia corroborating an earlier study by another group based on finite element calculations. In our analysis, the contact-resonances of the foot soles are exploited as a sign for surface contact. Because the acceleration data represent structure-borne sound in the foot soles in the audio range, they can be made audible in audio files which are attached to this publication.

1. Introduction

The landing of Philae, the Lander of the Rosetta mission, on comet 67P/Churyumov-Gerasimenko provided direct access to the surface elasticity and plastic deformation at the touchdown site Agilkia. The dynamics of the bouncing of Philae yielded an estimate of the comet surface compression strength of 1–3 kPa at the \sim 10 cm to 1 m scale [1]. A reconstruction of the touch-down events using a finite element simulation led to compression strength values from 1.5 to 1.8 kPa [2]. Analytical estimates based on the lander and landing gear dynamics led to 2 kPa for the compression strength [3]. Finally, modeling the soles of the feet as a damped contact oscillator coupled to the surface material of the comet, yielded for the compression strength 3.5-12 kPa [4]. The uncertainties of the values originated from (i) assumptions of the contact areas of the feet, (ii) whether the feet touched down simultaneously or sequentially, and (iii) whether a homogeneous or depth-dependent compression strength was assumed. The elastic modulus of the surface material was estimated from the compression strength [4,5] using empirical correlations between strength parameters, elasticity, and the porosity of materials which are well-known in material science [6].

In the present paper, we analyze the time evolution of the data of the accelerometers mounted in the foot soles of the landing gear using the short-time Fourier-transform (STFT). They yield the time sequence how the lander feet touched the comet's surface. The result is compared to the data of an earlier study by another group based on finite element calculations.

2. Landing event at Agilkia

Firstly, a brief account of the landing events as given by Biele et al. [1] is repeated here. On November 12th, 2014, the lander Philae was separated from the Rosetta orbiter. After 6:59:04 h of ballistic descent, Philae landed at the site Agilkia. The reconstruction showed that the velocity vector of the descent trajectory was 11.5 ± 1 deg away from the local normal. The touchdown speed relative to the comet surface was 1.012 m/s [2]. Furthermore, the central damping tube of Philae's landing gear was pushed in against the main lander body, generating the touchdown signal at 15:34:06.471 UTC with an uncertainty of \pm 1s [1]

E-mail address: w.arnold@mx.uni-saarland.de (W. Arnold).

https://doi.org/10.1016/j.actaastro.2025.03.044

^{*} Corresponding author.

and with a delay of a few seconds to the first signal of the Comet Acoustic Surface Sounding Experiment (CASSE). The stroke length of the damper in the landing gear was 42.6 \pm 0.1 mm out of a full length of $\sim\!170$ mm. Because the anchor harpoons did not fire upon touchdown and the hold-down thrust of the cold gas system did not work, the lander bounced several times until it came to rest at the site Abydos after about two more hours of ballistic flight.

The OSIRIS Narrow Angle Camera (NAC) images taken from the Rosetta orbiter were used together with ROLIS (Rosetta Lander Imaging System) descent images to determine the landing coordinates and the landscape at Philae's landing site Agilkia (Fig. 1a and b). Altitude and attitude of the lander with respect to the surface, and its rotational state were derived as well. The motion of the lander close to the surface of 67P comprised, besides the near vertical descent with a velocity of $v\approx 1$ m/s, also a counter-clockwise rotation around the main axis of the lander in top view with an angular frequency of $\omega\approx 1.26\times 10^{-2}\,\mathrm{s}^{-1}$ (0.72 deg/s) [1].

There are now several descriptions of the sequence of the landing events in relation to the various contacts of Philae with the comet surface [2,7–9].

3. Comet Acoustic Surface Sounding Experiment

The Comet Acoustic Surface Sounding Experiment (CASSE) was one of three instruments of the Surface Electric Sounding and Acoustic Monitoring Experiment (SESAME) on the lander Philae, which aimed at the determination of mechanical and electrical properties of the cometary nucleus and dust particles in the surroundings [10].

The operation principle of CASSE was to sound the comet's interior with elastic waves at frequencies of the order of a few kHz using piezoelectric transmitters and accelerometers mounted in the soles of the landing gear. A foot with two soles was attached to each of the three legs of the lander, one containing the transmitter and one the accelerometer (Fig. 2). Viewed from the outside, the transmitter is in the left sole, whereas the accelerometer is in the right sole. Parameters for the accelerometers are given in Ref. [10]. They were specially manufactured by Bruel & Kjaer (B&K) for the Rosetta mission and were based on miniature triaxial Deltatron accelerometer type 4506. Here, it is important to note that the transverse sensitivity (cross-talk sensitivity) is less than 5 % for the axis in question (see Product Data: High-sensitivity Triaxial CCLD Accelerometer Type 4506-B-003 (BP1838) (bksv.com)). CASSE was also used to listen to the hammering of the MUlti-PUrpose Sensors for Surface and Sub-Surface Science (MUPUS) penetrator into the cometary surface at the Abydos site [11] and additionally in order to

measure the acceleration of the landing shock and the sole's contact resonances when the feet touched ground on comet 67P at Agilkia [4].

The voltage signals of the accelerometers were amplified in CASSE electronics (16 different gains were adjustable by user command) and recorded with a 12-channel data recorder with a programmable sampling rate of up to 100 kHz. The conversion to digital units ("ADC units") was piecewise linear, approximating a logarithmic compression and thus allowing a larger amplitude range. A memory of 127 kB was available for storing the samples with the digital resolution of 7 bit plus sign. The duration of a typical measurement with the readout of all 9 accelerometer channels at a few kHz was therefore limited to a few seconds. When operating the instrument in space, additional memory constraints at SESAME and Philae level had to be considered which sometimes limited the measurement duration further.

4. Contact mechanics and contact resonances of the foot soles of Philae

Assuming a purely elastic contact, the interaction between the landing soles and the comet surface material is determined by a parameter called contact stiffness k^* (inverse of compliance):

$$k^* = 2E_r^* (A_c/\pi)^{0.5}$$
 . Eq. 1

Here, E_r^* is the effective modulus of the contacting materials, i.e., of the comet soil and that part of the landing gear which touches the surface, and A_c is the contact area. The quantity E_r^* contains the reduced elastic moduli of both contacting partners [12], here the comet soil $E_{r,c}$ and the foot soles $E_{r,sh}$:

$$1/E_r^* = 1/E_{r,c} + 1/E_{r,sh} = (1-v_c^2)/E_c + (1-v_{sh}^2)/E_{sh}$$
 Eq. 2

where E_c and E_{sh} are the corresponding elastic moduli and the Poisson ratios v_c and v_{sh} . From Eq. (1) it follows that in case of a sphere against a flat surface, entailing $A_c = \pi a_c^2$, the contact stiffness is given by

$$k^* = 2a_c E_r^*, Eq. 3$$

where a_c is the contact radius. Equation (1) is a very general relation that applies to any axisymmetric indenter. Although originally derived for elastic contacts, it has subsequently been shown to apply equally well to elastic–plastic contacts [13]. Furthermore, small perturbations from an axisymmetric geometry in the contacting materials do not change k^* much, and it is also unaffected by pile-up of the material and sink-in of the indenter. Both effects were observed at the landing site Agilkia [1].

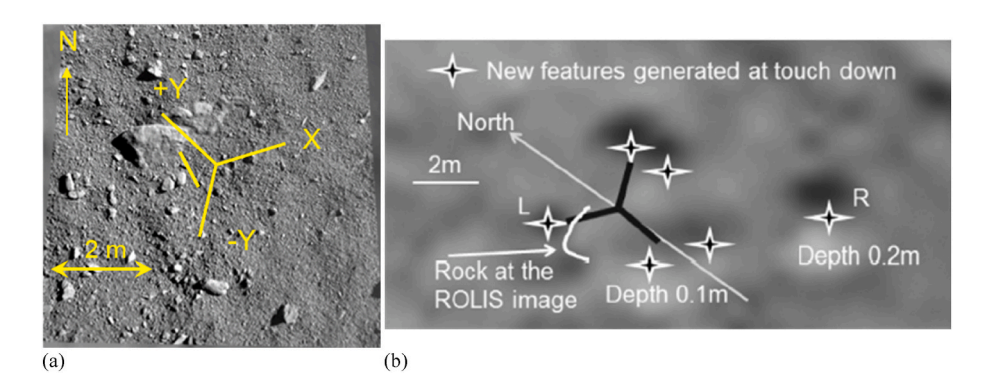


Fig. 1. (a) Lander position and orientation during Philae's first contact with the comet at the site Agilkia before landing. The lander legs are to scale and superimposed on merged and rectified ROLIS images. The yellow line indicates the lander balcony edge (see Fig. 2). The +Y leg hit the edge of the boulder seen near the center of the image. The resolution of the ROLIS image is 2 cm/pxl (full-resolution) and the positional uncertainty of Philae relative to the surface is ± 10 cm (in modified form from Ref. [4] with permission from Elsevier); (b) Projection of the position of the boulder from the ROLIS image in (a) onto the OSIRIS image. Additional features were produced by the lander touch-down. They are marked by star symbols. The letters L and R designate the most left, respectively the most right. The alignment accuracy between the ROLIS and the OSIRIS images was about 0.4 m (from Ref. [2] with permission from Elsevier). In the present paper we determine the time sequence of Philae contacts with the comet surface. (For interpretation of the references to color in this figure legend, the reader is referred to the Web version of this article.)

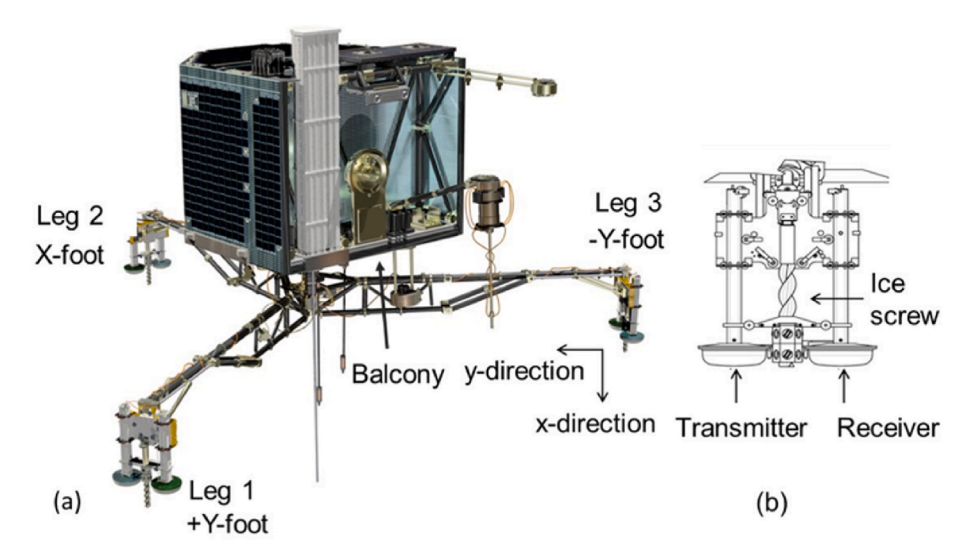


Fig. 2. (a) Definition of the Philae landing gear X, +Y, and -Y coordinate system and the accelerometer x-, y-, and z-directions. Leg 1 holds the +Y-foot, Leg 2 holds the X-foot, and Leg 3 holds the -Y foot. The coordinate system of each accelerometer is defined locally. The x-directions of all accelerometers in each of the right foot soles (seen from the outside) are positive downwards. The y-direction is parallel to the legs of the landing gear and positive inwards, whereas the z-direction is perpendicular to the x- and y-directions forming a right-handed coordinate system; (b) Double foot: The left sole houses the CASSE transmitter whereas the right sole houses a Brüel & Kjaer (B&K) triaxial accelerometer as receiver. The so-called "ice screws" served for the fixation of the lander on the comet soil. The width of the lander at the so-called "balcony" is 850 mm (in modified form from Ref. [4] with permission from Elsevier).

Viscous damping, friction and plastic deformation in the contact, requires that the contact stiffness k^* is a complex quantity $k^* = k_r + \mathrm{i} k_i$ [14] with $k_r = 2E_r^*(A_c/\pi)^{0.5}$ and $k_i = 2E_i^*(A_c/\pi)^{0.5}$. Consequently, the modulus $E^* = E_r^* + E_i^*$ becomes also complex, where E_i^* is the corresponding loss modulus. In our case, the contact radius a_c can be as large as the half-diameter of the sole, r, i.e., $a_c = r = 5$ cm.

The acceleration amplitudes of the landing shock and hence the forces acting between Philae's foot soles and the comet soil are determined on the one hand by the compliance of the material encountered at the landing location and, on the other hand, by the compliance of that part of the landing gear including the foot soles, which touched the surface [5]. Besides the absolute value of the force of the landing shock, the forced resonances of the soles of the feet can be used to obtain information on the local elastic modulus E and the compression strength σ_c of the comet soil [4]. The resonance frequencies of the soles depend on the contact stiffness and the oscillating mass involved. This has been evaluated by calibration experiments at the Landing & Mobility Test Facility (LAMA Tests) [15], and then applied to the landing of Philae at the site Agilkia. From the measured contact-resonances of the foot soles of the Philae lander's landing gear, the reduced modulus was determined [4]. Finally, there is dispersion of the resonance frequency versus contact stiffness or reduced elastic modulus (Eq. (3)) of the contacting partners because Philae's soles are mass-distributed oscillators.

To obtain the compression strength of the comet's surface material, one must determine the contact forces between the foot soles and the comet surface at the onset of plastic deformation and divide them by the contact area. The contact force was determined by solving the equation of motion of the foot soles [4]. As said above, this yielded a compression strength of 3.5–12 kPa.

5. Short-time fourier transform

Short-time Fourier transforms are mathematically represented as

$$STFT\left\{s(t)\right\} = S(\tau,\omega) = \int\limits_{-\infty}^{+\infty} s(t)\chi(t-\tau)e^{-j\omega t}dt$$
 Eq. 4

where s(t) is the signal in the time domain and $\chi(t)$ is a window function which is zero outside of a pre-determined duration and thus cuts out a

short part of s(t) beginning at time τ . To make the sampling of the signal quasi-continuous, the windows are overlapped by an amount called the skip distance. The quantity $|STFT(t,\omega)|^2$ is called the spectrogram of the signal. The choice of the window function leads to a trade-off between the time localization and frequency resolution. Short windows result in low frequency resolution, i.e. overlapping spectral peaks, while long windows provide better frequency resolution but do not allow precise assignment of frequency content to short signals [16]. The time-frequency resolution is $\Delta t\Delta\omega = \frac{1}{2}$ in case the window function is a Gaussian. The STFT are used in many fields. Applications in ultrasonic backscattering measurements for materials characterization are close to the applications discussed here [17,18].

Here, we applied the short-time Fourier transforms of the signals to evaluate the time sequence of the free and forced oscillations of the foot soles and thus the time evolution of the landing during the time intervals the accelerometers were switched on and received data, see Fig. 13. Only the first contacts at Agilkia could be recorded due to memory constraints.

The accelerometer signals were recorded with a rate of 5 kHz. Using the software OriginPro, the time series of 1800 ms length were divided into N=69 overlapping windows, each containing n=256 data points. The samples in each window were multiplied with a Hanning window $\chi(t)$. The shift of the next adjacent window for the STFT corresponded to 128 data points. Each interval is then Fourier transformed and the ensemble of STFT data is plotted as a function of time and frequency, see Fig. 3c - 11c. The spectrogram values are given in dB relative to the largest value recorded, which was 143.8 m/s² in the +Y foot in x-direction. The time intervals where the values in the moving window are zero are shown in white.

6. CASSE signals recorded at Agilkia

The Brüel & Kjaer (B&K) CASSE accelerometers were mounted in the foot soles such that the x-direction points perpendicular to their surfaces and hence into the comet soil, the y-direction parallel to the corresponding leg into the lander body, and the z-direction perpendicular to the x- and y-directions, forming a right-handed coordinate system, see Fig. 2. The designations of the feet can be seen in Fig. 2 as well. The B&K accelerometer signals in x-, y- and z-directions of the three feet and their

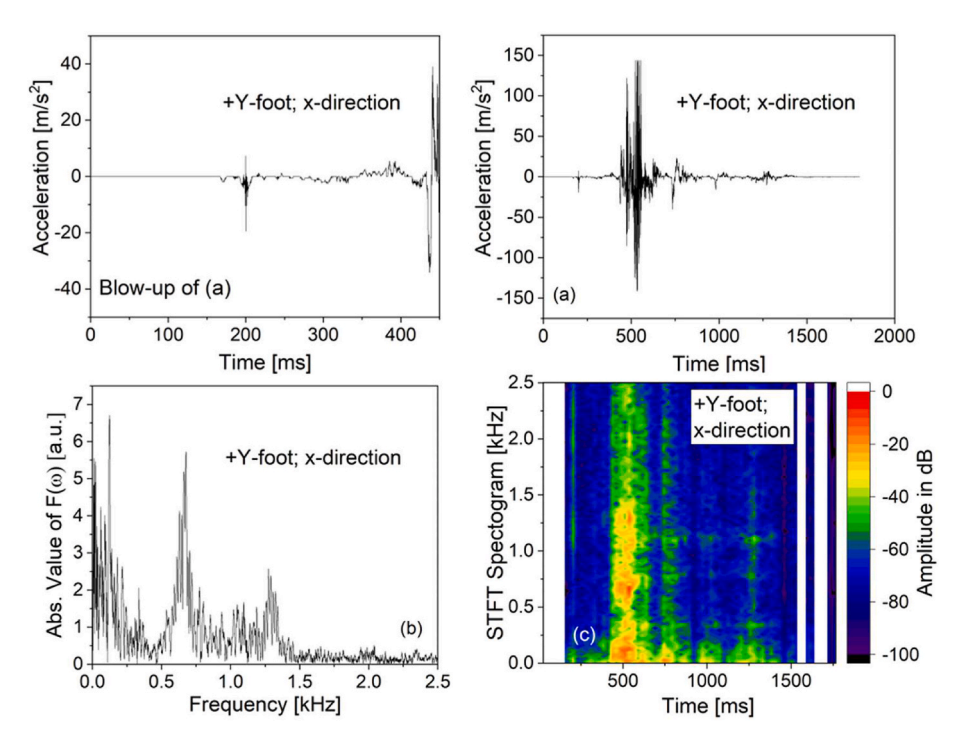


Fig. 3. Data measured by the accelerometer in the x-direction of the +Y-foot (Leg 1); (a) Acceleration data with enlarged portion showing the TD1 at 202 ms; (b) Fourier transform, and (c) Spectrogram of the short-time Fourier transform.

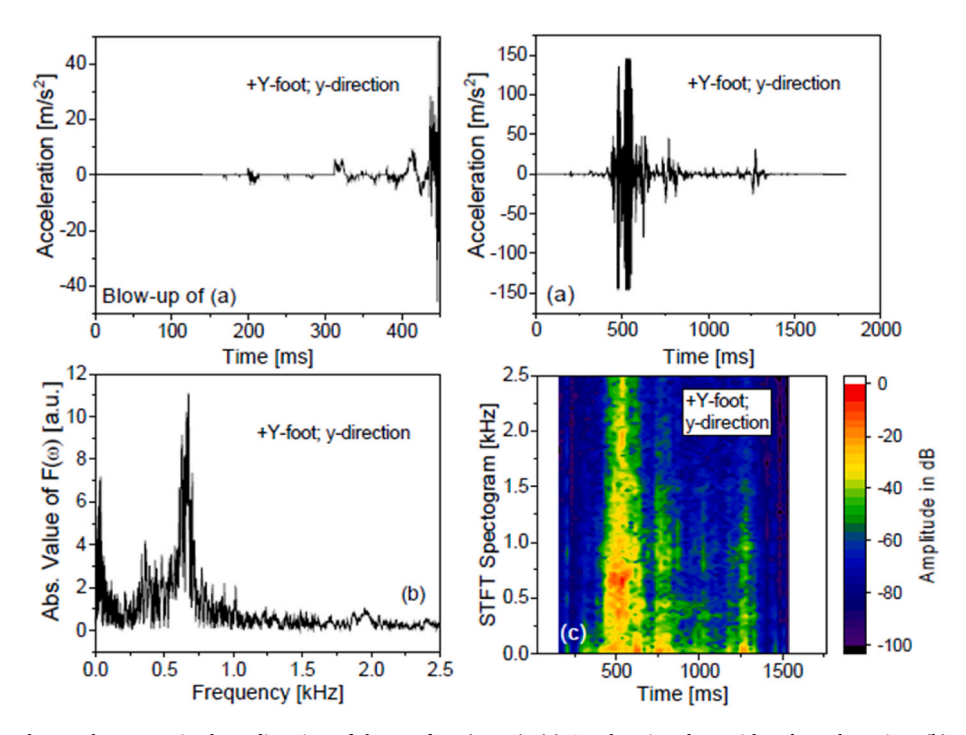


Fig. 4. Data measured by the accelerometer in the y-direction of the +Y-foot (Leg 1); (a) Acceleration data with enlarged portion; (b) Fourier transform, and (c) Spectrogram of the short-time Fourier transform.

Fourier-, respectively Short-Time Fourier-Transforms (STFT) are shown in Figs. 3–11.

Philae's first contact with the surface of 67P at Agilkia was a short "touch" of the +Y foot (Leg 1), see signals at $t=202\pm3$ ms in all three directions x, y, and z (blow-ups of Fig. 3a, 4a and 5a). This signal occurred at 15.34:03.98 \pm 0.1 s UTC [1] and is called TD1, the first touchdown at the site Agilkia. The signal strengths are weak in view of the later amplitudes at t>450 ms (Fig. 3a, 4a and 5a). The TD1 signal in

y- and z-direction (3 to $-4\,\text{m/s}^2$, respectively +8 to $-4\,\text{m/s}^2$) are smaller than the one in x-direction (+8 to -19 m/s 2). Both are followed by sawtooth-like negative excursions which are most likely due to the amplitude discretization steps ($\pm 0.6\,\text{m/s}^2$). No corresponding signals in the same time interval were detected by the other accelerometers in the X- and -Y feet.

From the appearance and the amplitude of the signals it becomes clear that the X (Figs. 6-8) and -Y feet (Figs. 9-11) encountered the

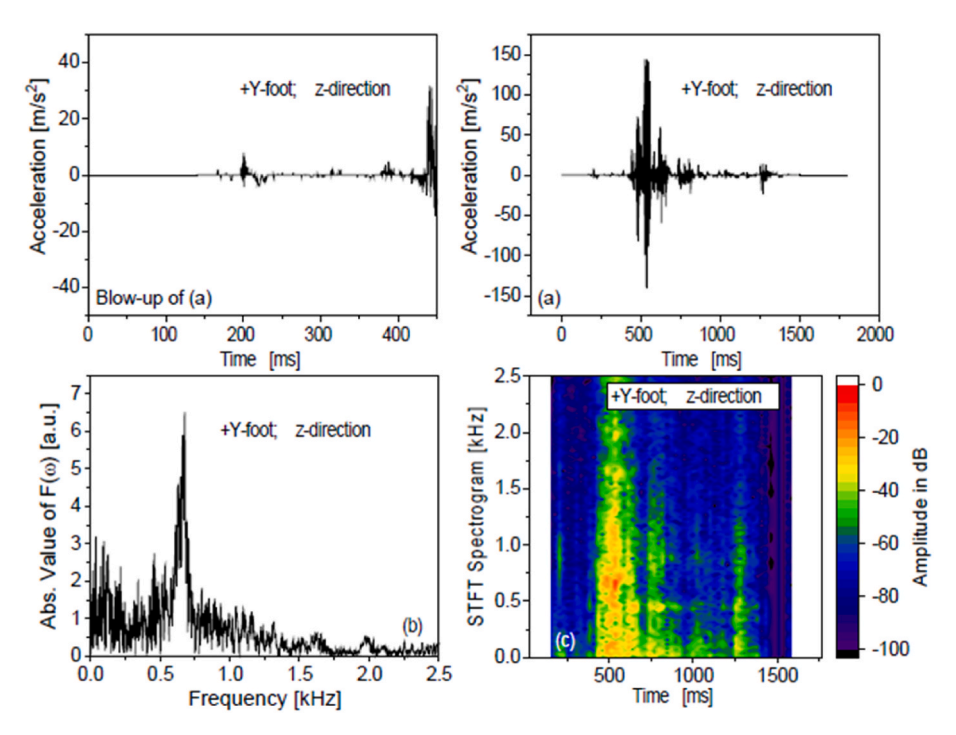


Fig. 5. Data measured by the accelerometer in the z-direction of the +Y-foot (Leg 1); (a) Acceleration data with enlarged portion; (b) Fourier transform, and (c) Spectrogram of the short-time Fourier transform.

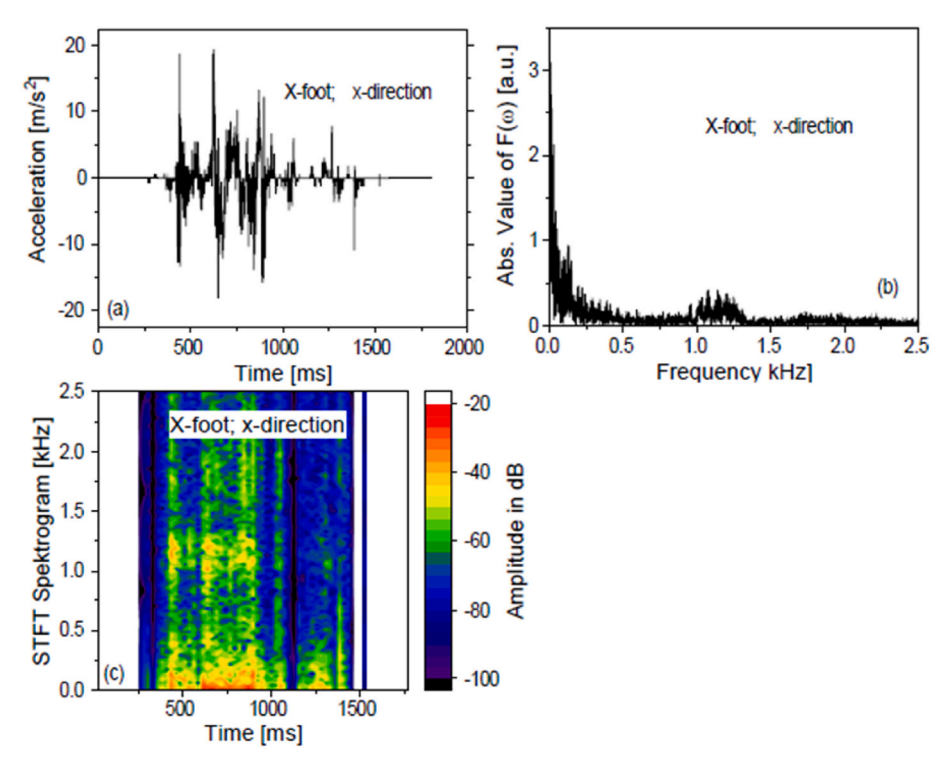


Fig. 6. Data measured by the accelerometer in the x-direction of the X-foot (Leg 2); (a) Acceleration data; (b) Fourier transform, and (c) Spectrogram of the short-time Fourier transform.

comet surface in a different way from that of the +Y-foot (Figs. 3–5). The +Y-foot experienced negative (upward movement) and positive amplitudes (downward movement) exceeding $\pm 140~\text{m/s}^2$ (saturation level) in all three accelerometer directions, whereas the X-foot experienced values of maximum accelerations in the three accelerometer directions of $\pm 20~\text{m/s}^2$ (x-direction), 30 to – 40 m/s² (y-direction); 40 to -20 m/s² (z-direction). For the –Y foot these values are $\pm 40~\text{m/s}^2$ (x-

direction), 35 to - 20 $\mbox{m/s}^2$ (y-direction), and 40 to - 50 $\mbox{m/s}^2$ (z-direction).

Also, the Fourier spectra are quite distinct. Firstly, all three feet show low-frequency signals below 0.5 kHz. Secondly, there are frequency groups much above noise at 0.67 kHz for the +Y foot in the x-, y-, and z-directions (Fig. 3b, 4b and 5b). In the x-direction (Fig. 3b), a frequency band appears additionally at ≈ 1.35 kHz. For the X-foot (Figs. 6–8) and

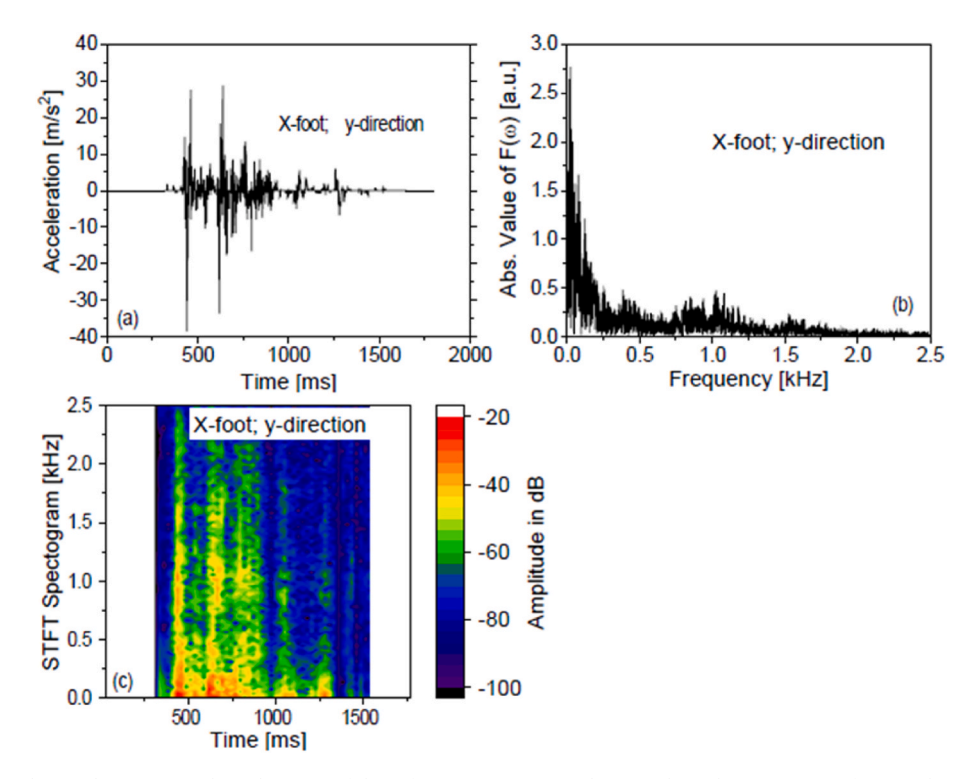


Fig. 7. Data measured by the accelerometer in the y-direction of the X-foot (Leg 2); (a) Acceleration data; (b) Fourier transform, and (c) Spectrogram of the short-time Fourier transform.

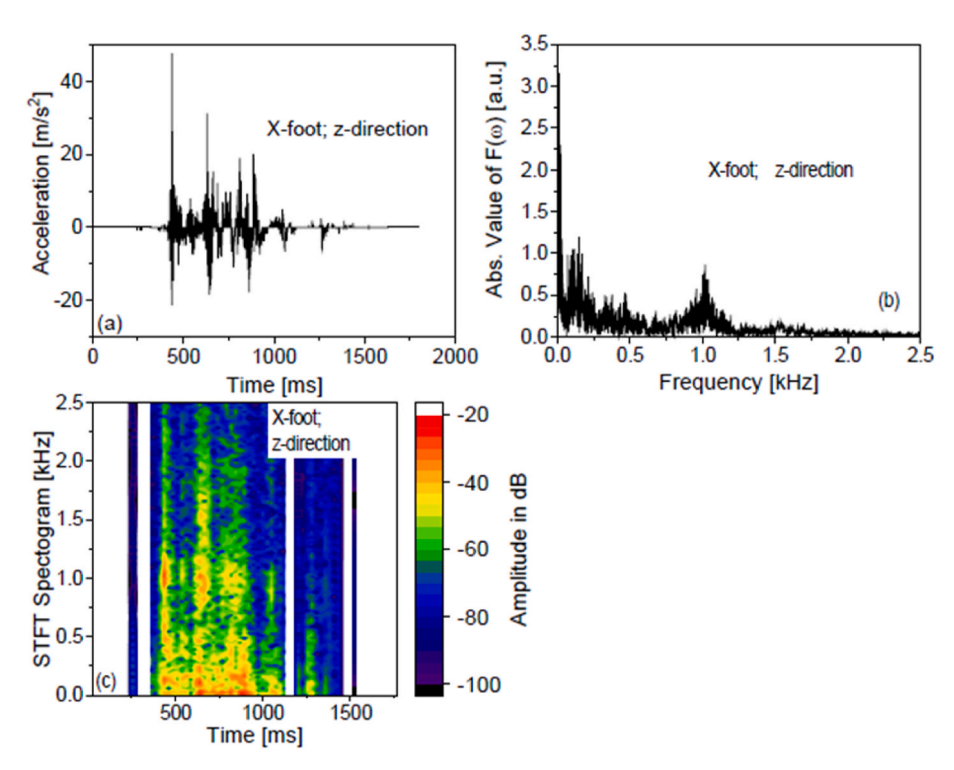


Fig. 8. Data measured by the accelerometer in the z-direction of the X-foot (Leg 2); (a) Acceleration data; (b) Fourier transform, and (c) Spectrogram of the short-time Fourier-transform.

for the -Y-foot (Figs. 9–11), there are frequencies above the noise at $\approx 0.9–1.3$ kHz. The fact that both signs occur in these signals means that the soles of the Philae feet, which housed the accelerometer, were excited to oscillations when encountering the comet surface.

7. Data analysis

7.1. Time delay of the first touch-down signal relative to the main signal From the shadow of the boulder, its height was determined to be $h \approx$

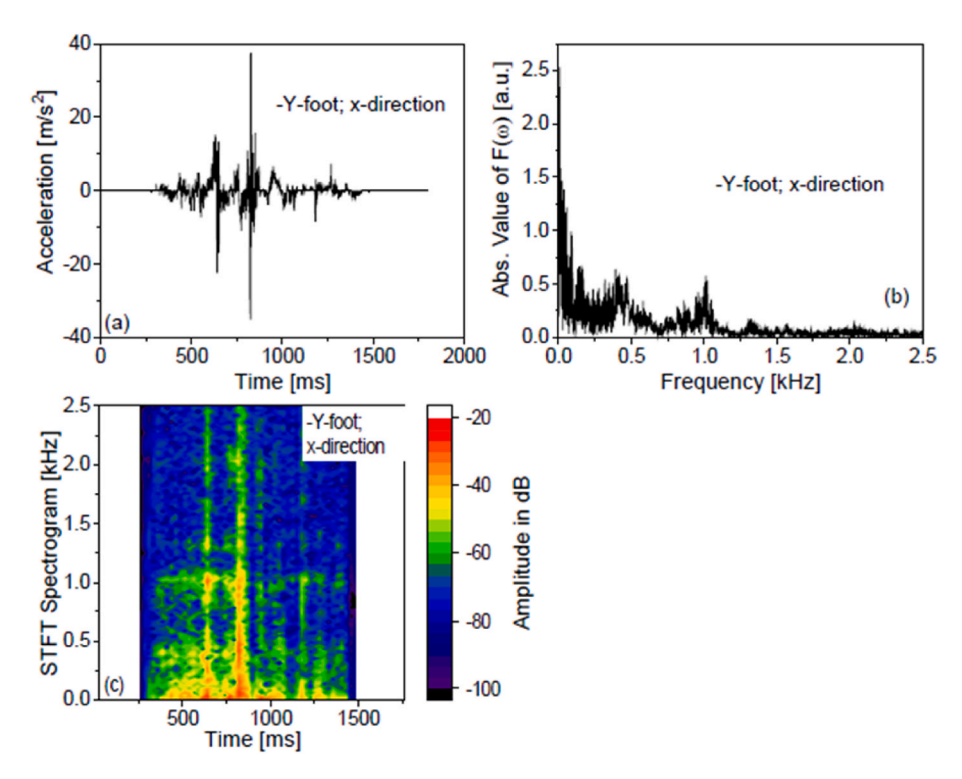


Fig. 9. Data measured by the accelerometer in the x-direction of the -Y-foot (Leg 3); (a) Acceleration data; (b) Fourier transform, and (c) Spectrogram of the short-time Fourier transform.

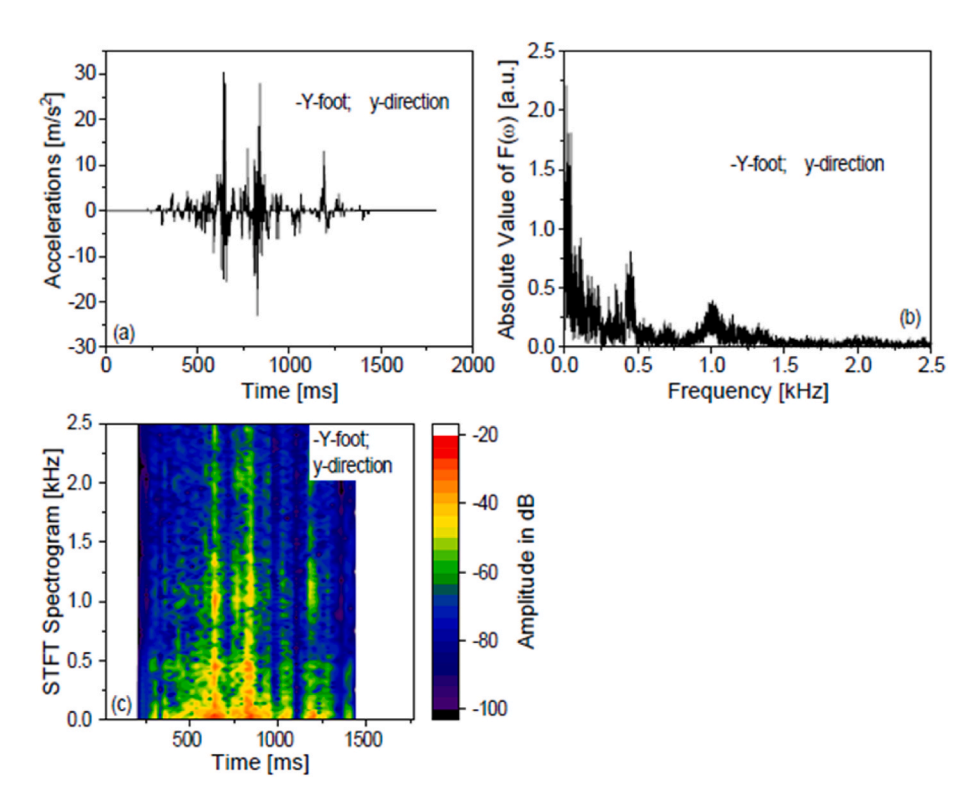


Fig. 10. Data measured by the accelerometer in the y-direction of the -Y-foot (Leg 3); (a) Acceleration data; (b) Fourier transform, and (c) Spectrogram of the short-time Fourier transform.

0.34 m on one side of the boulder (left side in Fig. 12) [4]. The boulder's edge gently merged into the surface of the comet on the other side. The distance d from the foot sole to a cross strut is \approx 0.18 m as measured on a flight-identical component. Thus, the time difference between the first small signal in the +Y-foot in x-direction at t=202 ms and the onset of

the first main signal at $t\approx 435$ ms (negative excursions in Figs. 3a, 4a, and 5a and blow-ups) was likely caused by the delay due to the sink velocity of Philae of 1.012 m/s, yielding a travel distance of ≈ 0.24 m before the strut hit the edge of the boulder, in reasonable agreement with the clearance of 0.18 m. As said above, the signals in y- and

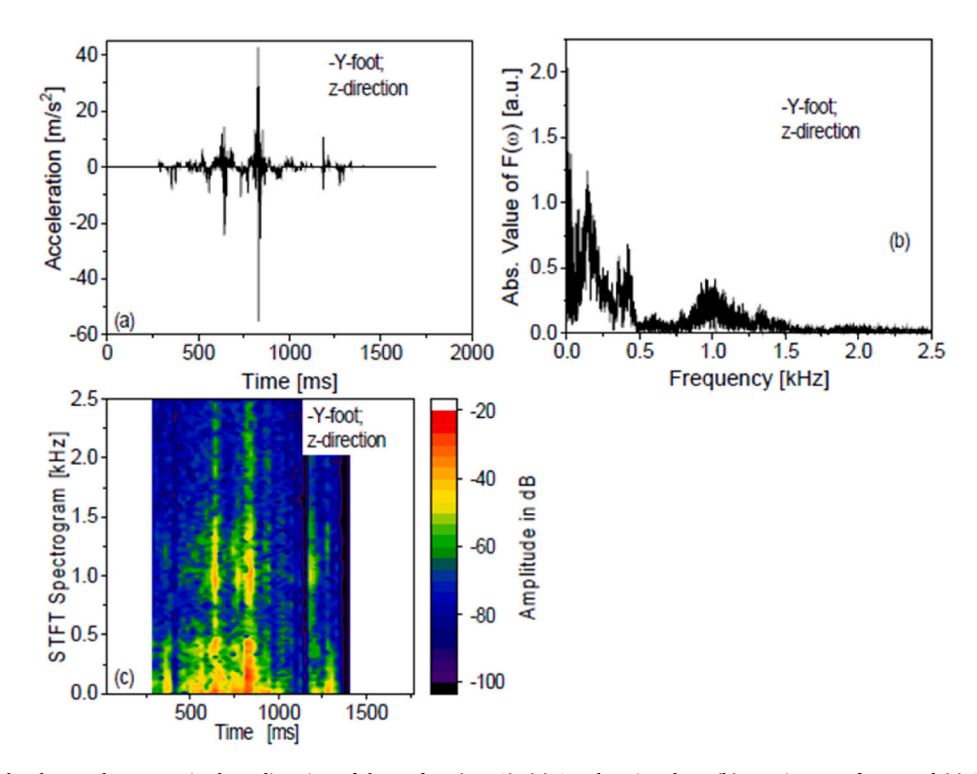


Fig. 11. Data measured by the accelerometer in the z-direction of the -Y-foot (Leg 3); (a) Acceleration data; (b) Fourier transform, and (c) Spectrogram of the short-time Fourier transform.

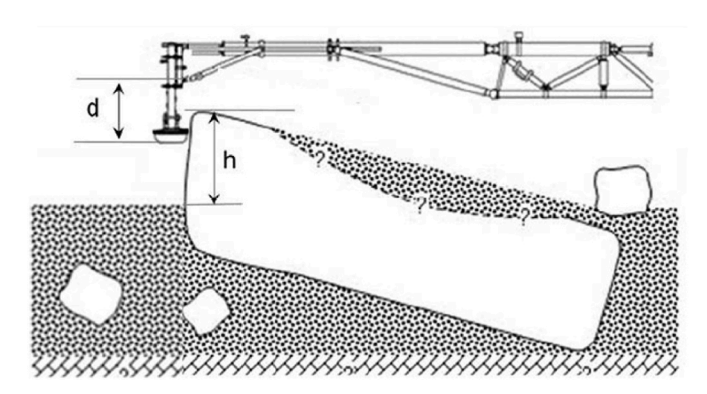


Fig. 12. Scenario of the touchdown for the +Y-foot at the landing site Agilkia (in modified form from Ref. [4] with permission from Elsevier). The distance foot-sole to strut of the landing gear is $d\approx 0.18$ m and the height of the boulder $h\approx 0.34$ m.

z-direction (3 to -4 m/s^2 , respectively $+8 \text{ to } -4 \text{ m/s}^2$) are smaller than the one in x-direction ($+8 \text{ to } -19 \text{ m/s}^2$), reflecting the amplitudes of the forces acting on the soles which were all above the cross-talk threshold of 5%. The strong signals in all three accelerometer directions in the +Y-foot were caused when the strut hit the edge of the boulder, see Figs. 3a, 4a and 5a. Finally, the +Y-foot hit ground (Fig. 1b) exciting the contact-resonances of the foot-soles. Because the strut was much stiffer than the boulder, the force exerted by the strut on the boulder most likely exceeded its compression strength leading to the boulder's collapse and to the excavation of the hole L in Fig. 1b.

The accelerometers in the X-foot were excited at $t\approx 435$ ms to oscillations in all three directions as well, see Fig. 6a, 7a and 8a as they touched ground (Fig. 1b). However, the amplitudes (peak-to-peak) are reduced by a factor ≈ 3 –6 compared to the values of the +Y foot. For the -Y foot the situation is different, because the signal strength at t=435 ms is only ≈ 1.5 m/s 2 in all three directions (Fig. 9a, 10a and 11a), i.e. a factor of 100 reduced compared to the +Y foot.

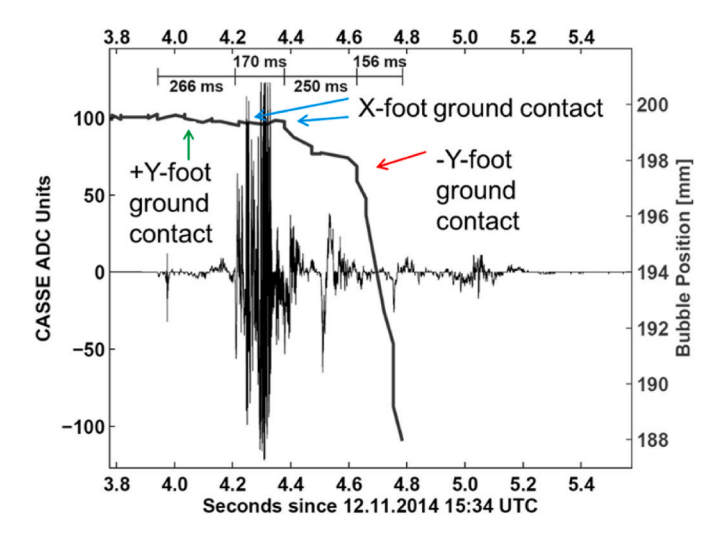


Fig. 13. Damper potentiometer reading at touch-down (right scale) superimposed with the CASSE + Y foot signal (left scale, uncalibrated). The damper movement starts at $15:34:03.98\pm0.1s$ for a period of 266 ms. In this window, the first signal of the CASSE accelerometer mounted in the +Y-foot was detected (green arrow). At 15:34:04.62 (marked "-Y-foot ground contact", red arrow) the movement of the lander damper was more pronounced as compared to its motion indicated by the blue arrows (X-foot ground contact). The strong CASSE signals in x-direction were not accompanied by a simultaneous damper movement. The acceleration data in this figure correspond to the calibrated data shown in Fig. 3a. In modified form from Ref. [1] with permission from AAAS; see also [3]. (For interpretation of the references to color in this figure legend, the reader is referred to the Web version of this article.)

7.2. Analysis of the Signal's Fourier and short-time Fourier transforms

Figures 3b to 11b display the Fourier transforms of the landing signals of all three feet in the x-, y-, and z-directions. The +Y-foot shows strong oscillations at 0.67 kHz in the x-, y-, and z-direction. The

spectrogram shows a frequency band in the x-direction from about 0.5 kHz to 1.4 kHz with maximum values at 0.67 kHz (\sim 25 dB read from the color scale), and at 1.32 kHz (\sim 20 dB). For the y- and z-directions, the spectrogram maximum at 0.67 kHz corresponds to 26 dB and 25 dB, respectively. The spectrogram power is then decreasing with some smaller maximum values up to 2.5 kHz. The behavior of the X-foot and the -Y-foot is quite different. Here, besides frequencies below 0.5 kHz, there are frequency bands from \sim 1–1.3 kHz in all three directions (–1 dB). The latter can be clearly discerned in the STFT from 420 ms onwards for the X-foot and about 620 ms onwards for the -Y-foot. For the +Y-foot, the strong signals at 0.67 and 1.32 kHz are localized between approximately 440 and 550 ms, as can be seen in the STFT plot (Fig. 3c). The time span between TD1 and 440 ms, i.e. approximately 240 ms corresponds again to the path length $d \approx 0.24$ m where the foot scratched along the boulder (Fig. 12).

Calibration experiments showed that the free resonance frequency of two different flight-spare foot-soles were 0.5 kHz and 0.6 kHz, respectively [15,19]. For the actual flight model a free resonance frequency of 0.641 kHz was measured during the cruise phase [20]. Thus, we assign the signal of the +Y-foot at 0.67 kHz as its free resonance excited by scratching sidewise along the backside of the boulder (Fig. 12). Furthermore, the signal at 1.1 kHz has been interpreted as a contact-resonance frequency [4] when the sole finally touched ground several times from about 500 ms onward to 1.4 s as can be seen from the STFT in Fig. 3c (orange and green spots). Their amplitudes are weaker than the amplitude of the free resonance at 0.67 kHz, at least by 10 dB as can be seen from Figs. 3b and c.

For the X- and -Y foot, there are signals between 1.1 and 1.32 kHz. For the X-foot, these occur in the STFT at about 420 ms, at \approx 650 ms, and at \approx 850 ms (Figs. 6c, 7c and 8c), agreeing with the time-position of the amplitude peaks shown in Figs. 6a, 7a and 8a. For the -Y foot, the FFT of Fig. 9b shows signals at 1.0 kHz and the STFT (Fig. 9c) indicates that they occur at the same times as the two amplitude peaks in the timeseries. These signals are delayed relative to the two other feet. Using the same argument as above, they can be interpreted as the sole's contact-resonances with the pebbles of the comet surface material. As proposed earlier [4], these signal groups reflect individual contacts with the comet surface due to the motion of the lander, the induced oscillations of the landing leg, the local terrain, and the partial deployment of the ice screw [3]. The time-delay of the individual signal groups in the time-series (Fig. 3a - 11a) relative to the first signal were also observed in laboratory landing tests and were caused by the effects just mentioned [15]. The distribution of frequencies was caused by varying contact stiffnesses. Either the contact area, due to the size distribution of the pebbles as described by Motolla et al. [21], or the elasticity distribution due to varying porosities of the pebbles can be the origin of the contact stiffness leading to frequency bands, see Eqs. (1) and (3). This holds also for the sidewise scratching as it changes the boundary condition of the foot-sole oscillator and hence its eigenfrequency. The signal at 1.32 kHz in the x-direction may also be interpreted as its first harmonic due to the higher order elastic constants of the sole's glass-fiber composite material [22].

From the STFT, the Fourier transforms, and the time series of the signals, one can conclude that the lander Philae first touched the boulder on its backside with the +Y-foot sole containing the accelerometer. Then, for about 180 ms the descent continued until Leg 1 (+Y-foot) and Leg 2 (X-foot) touched the surface at the same time, followed by Leg 3 (-Y-foot) after a further delay of 210 ms. Finally, the lander made a complicated sequence of motions which has been examined by Roll and collaborators using finite element analysis. At the time of their analysis only the acceleration data from Leg 1 (+Y-foot) in x-direction and data from the landing gear were at their disposal, see Refs. [2,3]. The results are summarized in the next chapter.

Finally, vibration frequencies below 0.5 kHz have been observed in the LAMA calibration and landing tests as well and were interpreted as structural oscillations of the various parts of the landing gear [15]. We checked this interpretation by re-analyzing the LAMA test data. The ensemble of the signals shown in these files resembles very much the signals measured on the comet soil, particularly the occurrence below 0.2 kHz. However, one has to keep in mind that the Young's moduli of the LAMA test materials (MSS and W34 sands) are at least an order of magnitude higher than the elastic modulus of the regolith material on the comet surface [4]. Some of the LAMA test data are shown in the Supplementary Files.

7.3. Time sequence of the surface contacts of Philae's legs 1-3 at Agilkia

As said above, simulations were performed using a FEM analysis with a dedicated mechanical multi-body model of the lander by Roll and Witte [2]. They focused on the reconstruction of Philae's touch-down at Agilkia from the first ground contact to lift-off again. The input data were the pattern on ground documented by the OSIRIS Narrow Angle Camera (NAC) (Fig. 1b), the inbound and outbound velocity of the lander for the first touch-down at site Agilkia [1], and other lander data.

The FEM modeling showed that the lander had repeated contacts with the surface over a period of about 20 \pm 10 s. Furthermore, the simulation showed that the outbound velocity vector and the lander rotation were formed immediately at touch-down during the first 1.5 s, i. e. during the time interval in which the accelerometers in the feet captured the signals shown in Figs. 3–11. The outbound velocity vector was determined by the ground slope and the lander damping characteristic, especially the nearly horizontal flight out. The modeling resulted in a compressive strength of the soil of 1.55–1.8 kPa for foot 2 and 3 and 18 kPa for foot 1. The friction coefficients between the soles and the comet soil, assumed to be 0, 0.5, and 1, influenced these values. However, the influence on the outgoing velocities v_z , v_x , and v_y , and the ensuing lander rotation and nutation was more pronounced. The same holds for an assumed lateral ground strength of 10 Pa. Also, the consequences of a depth dependent compression strength was considered by Roll and Witte [2].

In a further work, Roll et al. [3] examined in detail the forces within the landing gear in order to obtain the forces of the foot soles exerted on the comet soil. If the force F acted on a foot to penetrate the comet surface material in a plastic manner, then the quotient F/A, where A is the foot area, is its compressive strength. Considering the energies dissipated by the lander damper and by the plastic deformation of the comet soil by creating the excavations [1] (Fig. 1b), an average force of 34 N was adopted for each foot. This entailed a compressive strength $\sigma = F/A \approx 2$ kPa with F = 34 N and A = 0.017 m² for the two soles of each foot. This estimate was obtained from data for the first 200 ms of the motion of the damper before the legs of the landing gear entered the ground significantly, and for a depth-independent compression strength.

The combination of data from the FEM [2] and analytical modeling [3] of the landing event led to the conclusion, that the +Y foot mounted on Leg 1 hit the comet ground first (TD1), followed by the X-foot mounted on Leg 2, and then by the -Y-foot (Leg 3) over a time range of up to 0.6 s [3].

This sequence of events is fully corroborated by the results obtained from the STFT analysis (Fig. 13). The arrow in green marks the first contact which occurred at 15:34:03.98 \pm 0.1s (+Y-foot ground contact, TD1), corresponding to the signal at $t=200~\rm ms$ in the blow-up of Fig. 3a (amplitude +8 to $-19~\rm m/s^2$). These signals were observable in the +Y-foot in the y- (3 to -4 m/s²) and z-directions as well (8 to -4 m/s²) (blow-ups of Fig. 4a and 5a). However, they could not be observed in the X-foot nor in the -Y foot in the x-, y- and z-directions. The time windows of different lengths (266, 170, 250, and 156 ms) in Fig. 13 were first discussed in Ref. [1] and assigned to different damper motions. From the present STFT analysis one can assign the damper motions to the surface contact of the landing gear's feet (green, blue, and red arrows). They are characterized by the contact-resonance oscillations of the foot-soles at 1.1–1.3 kHz, see the corresponding STFT spectrograms.

8. Audio signals

The acceleration data shown in Figs. 3–11 have been converted to audio signals in the MP4 format. The audio signals represent the structure-borne sound generated by the oscillations of the foot-soles when in contact with the comet surface.

When playing the files (see supplementary material), one can clearly hear the strong sound-pulse encompassing different frequencies according to the STFTs shown in Figs. 3c to 5c in agreement with the timeseries of the signals shown in Figs. 3a, 4a and 5a. They are followed by two weaker signals. In the background one hears a scratching noise. In the audio files corresponding to Fig. 6c, 7c and 8c, one can hear from the pitch of the tone as a function of time the varying frequency content corresponding to the contact resonances of the foot soles. For example, when playing the audio file of the X-foot in the x-direction signal (Fig. 6a), one can hear the three main signals having the same pitch followed by a tone reminding of scratching. This is also reflected in the FFT and the STFT data (Fig. 6b and c). The audio data of the -Y-foot can be interpreted in an analogous way.

9. Summary

The CASSE data from the landing of Philae at Agilkia presented here support the interpretation that the first contact at t=200 ms was a gentle sidewise touch of the +Y-foot at the backside of the boulder seen in Fig. 2 and was caused by the scratching of the edge of the foot sole with the back-side of the boulder.

The strong CASSE signals shown in Fig. 3a-5a were initially not caused by large forces attacking the sole of the +Y-foot. These signals were quasi-free vibrations of the foot soles without ground contact as evidenced by the STFTs shown in Fig. 3c-5c. Eventually the strut of the leg of the +Y-foot hit the boulder, causing the strong signals in the y- and z-directions of the +Y-foot, most likely leading to the boulder's destruction. Only then the +Y-foot hit ground. Furthermore, the delayed on-set of the contact-resonance oscillations of the X-foot and the -Y foot supports the analysis that they touched the comet surface with a delay relative to the +Y-foot which caused further damper movement (blue and red arrows in Fig. 13). Thus, the STFT results confirm the earlier interpretation of the landing data [2,3]. Finally, the audio signals presented here complement the above analysis.

CRediT authorship contribution statement

W. Arnold: Writing – original draft, Methodology, Data curation, Conceptualization. M.M. Becker: Writing – review & editing, Formal analysis, Data curation. H.-H. Fischer: Writing – review & editing, Formal analysis, Data curation. B. Ibrahim: Writing – review & editing, Software, Data curation. M. Knapmeyer: Writing – review & editing, Formal analysis. H. Krüger: Writing – review & editing, Formal analysis.

Declaration of competing interest

The authors declare that there is no conflict of interest regarding the publication of this article.

Acknowledgement

We thank Dr. V. Pfahl, from Fagus-GreCon Greten GmbH & Co. KG, Alfeld, Germany, for converting the time-series signals into audio files. One of us (W.A.) thanks Dr. Anish Kumar and Dr. Govind Sharma, both from the Indira Gandhi Center for Atomic Research, Kalpakkam, India for helpful discussions concerning the use and application of the STFT transform. Furthermore, we thank W. Gebhardt and R. Licht for their invaluable contributions in developing the CASSE instrument at Fraunhofer IZFP.

Two of us (M. M. B. and I. B.) thank the Fraunhofer Society for partial

support by the Internal Funding Program "Attract" under No. 025-601314.

Rosetta was an ESA mission with contributions from its member states and NASA. Rosetta's Philae lander was provided by a consortium led by DLR, MPS, CNES and ASI. SESAME was an experiment on the Rosetta lander Philae. It consisted of three instruments CASSE, DIM and PP, which were provided by a consortium comprising DLR, MPS, FMI, MTA EK, Fraunhofer IZFP, Univ. Cologne, LATMOS and ESTEC. All data are available via the ESA Planetary Science Archive.

Appendix A. Supplementary data

Supplementary data to this article can be found online at https://doi.org/10.1016/j.actaastro.2025.03.044.

References

- [1] J. Biele, S. Ulamec, M. Maibaum, R. Roll, L. Witte, E. Jurado, et al., The landing(s) of Philae and inferences about comet surface mechanical properties, Science 349 (2015). https://doi.org/10.1126/science.aaa9816 aaa9816 ARTN aaa9816.
- [2] R. Roll, L. Witte, ROSETTA lander Philae touch-down reconstruction, Planet. Space Sci. 125 (2016) 12–19, https://doi.org/10.1016/j.pss.2016.02.005.
- [3] R. Roll, L. Witte, W. Arnold, ROSETTA lander Philae soil strength analysis, Icarus 280 (2016) 359–365, https://doi.org/10.1016/j.icarus.2016.07.004.
- [4] D. Möhlmann, K.J. Seidensticker, H.-H. Fischer, C. Faber, A. Flandes, M. Knapmeyer, et al., Compressive strength and elastic modulus at Agilkia on comet 67P/Churyumov-Gerasimenko derived from the CASSE touchdown signals, Icarus 303 (2018) 251–264, https://doi.org/10.1016/j.icarus.2017.09.038.
- [5] W. Arnold, D. Möhlmann, Strength of comet material and hertzian contactmechanics applied to the landing of Philae on comet Churyumov-Gerasimenko, Aerotechnica, Missili & Spacio, J. Aerosp. Sci. Technol. Syst. 88 (2009) 145–149.
- [6] L.J. Gibson, M.F. Ashby, The mechanics of 3-dimensional cellular materials, Proceedings of the Royal Society of London Series a-Mathematical Physical and Engineering Sciences 382 (1982) 43–51, https://doi.org/10.1098/rspa.1982.0088.
- [7] P. Heinisch, H.U. Auster, B. Gundlach, J. Blum, C. Guttler, C. Tubiana, et al., Compressive strength of comet 67P/Churyumov-Gerasimenko derived from Philae surface contacts, Astron. Astrophys. 630 (2019), https://doi.org/10.1051/0004-6361/201833889. A2-1-8 A2.
- [8] L. O'Rourke, P. Heinisch, J. Blum, S. Fornasier, G. Filacchione, H. Van Hoang, et al., The Philae lander reveals low-strength primitive ice inside cometary boulders, Nature 586 (2020) 697–701, https://doi.org/10.1038/s41586-020-2834-3.
- [9] X.Y. Wu, M. Kuppers, B. Grieger, H.B. Shang, Characterization of the Agilkia region through discrete-element simulation of Philae's rebound, Astron. Astrophys. 630 (2019), https://doi.org/10.1051/0004-6361/201834843. A14 1-14 A14.
- [10] K.J. Seidensticker, D. Moehlmann, I. Apathy, W. Schmidt, K. Thiel, W. Arnold, et al., SESAME an experiment of the Rosetta lander Philae: objectives and general design, Space Sci. Rev. 128 (2007) 301–337, https://doi.org/10.1007/s11214-006-0118-6
- [11] M. Knapmeyer, H.-H. Fischer, J. Knollenberg, K.J. Seidensticker, K. Thiel, W. Arnold, et al., The SESAME/CASSE instrument listening to the MUPUS PEN insertion phase on comet 67P/Churyumov-Gerasimenko, Acta Astronaut. 125 (2016) 234–249, https://doi.org/10.1016/j.actaastro.2016.02.018.
- [12] K.L. Johnson, Contact Mechanics, Cambridge University Press, Cambridge UK,
- [13] W.C. Oliver, G.M. Pharr, Measurement of hardness and elastic modulus by instrumented indentation: advances in understanding and refinements to methodology, J. Mater. Res. 19 (2004) 1–20, https://doi.org/10.1557/ imr 2004 0002
- [14] P.A. Yuya, D.C. Hurley, J.A. Turner, Contact-resonance atomic force microscopy for viscoelasticity, J. Appl. Phys. 104 (2008), https://doi.org/10.1063/1.2996259, 074916-1-7 ARTN 074916.
- [15] C. Faber, M. Knapmeyer, R. Roll, B. Chares, S. Schröder, L. Witte, et al., A method for inverting the touchdown shock of the Philae lander on comet 67P/Churyumov-Gerasimenko, Planet. Space Sci. 106 (2015) 46–55, https://doi.org/10.1016/j. pss.2014.11.023.
- [16] J.L. Rose, Ultrasonic Waves in Solid Media, Cambridge University Press, Cambridge, UK, 1999.
- [17] G.K. Sharma, A. Kumar, C.B. Rao, T. Jayakumar, B. Raj, Short time Fourier transform analysis for understanding frequency dependent attenuation in austenitic stainless steel, NDT E Int. 53 (2013) 1–7, https://doi.org/10.1016/j. pdteint.2012.09.001
- [18] Y.G. Bu, X.L. Liu, J.A. Turner, Y.F. Song, X.B. Li, Grain size evaluation with time-frequency ultrasonic backscatter, NDT&E Int. 117 (2021) 102369, https://doi.org/10.1016/j.ndteint.2020.102369.
- [19] W. Arnold, R. Roll, Calibration Measurement of the Sole Contact-Resonances Carried out at the MPS-MPI, unpublished, Göttingen, 2015.

- [20] K.J. Seidensticker, H.-H. Fischer, W. Schmidt, A. Hirn, Philae Payload Checkout 13, Cruise Phase Report, 2012, p. 40,. DLR, Cologne, Germany.
- [21] S. Mottola, G. Arnold, H.G. Grothues, R. Jaumann, H. Michaelis, G. Neukum, et al., The structure of the regolith on 67P/Churyumov-Gerasimenko from ROLIS descent imaging, Science 349 (2015) aab0232, https://doi.org/10.1126/science.aab0232.
- [22] S.K. Chakrapani, Nonlinear laminated plate theory for determination of third order elastic constants and acoustic nonlinearity parameter of fiber reinforced composites, Compos. Struct. 180 (2017) 276–285, https://doi.org/10.1016/j. compstruct.2017.08.009.